Immense tunnel magnetoresistance mediated by Coulomb blockade effect and current-driven magnetization reversal in Co clusters embedded in a TiO_2 matrix

J. Varalda[1], D. H. Mosca[2], Y.-L. Zheng[3], A. J. A. de Oliveira[1], M. Marangolo[3,] W. A. Ortiz[1], D. Demaille[3], B.Vodungbo[3] and V. H. Etgens[3]

[1] Departamento de Física – UFSCar, C. P. 676, 13565-905 São Carlos SP, Brazil

[2] *Departamento de Física – UFPR, C. P. 19091, 81531-990 Curitiba PR, Brazil*

[3] *INSP, Institut des NanoSciences de Paris, UMR CNRS 7588, Universités Paris 6 et Paris 7 Campus Boucicaut – 140 rue de Lourmel – 75015 Paris, France*

Abstract: Magnetic and magneto-transport properties of Co nanoclusters embedded in a $TiO_{2-\delta}$ matrix grown by pulsed laser ablation have been studied. The results show a tunneling magnetoresistance (TMR) as high as 300%, associated with spin-polarized multiple quantum tunneling through the Coulomb energy barrier (Coulomb blockade effect). The interplay between the Coulomb blockade effect and the magnetization reversal driven by spin-polarized tunneling currents has been evidenced to occur concomitantly with a immense variation of the TMR.

PACS: 72.25.-b, 73.23.Hk, 73.40.Gk, 73.40.Rw, 73.63.-b

The milestone of the emerging spintronic technology is the use of the spin degree of freedom in charge-based electronics. A new generation of devices has been concieved and developed, devoted to combine standard microelectronics with spin dependent effects which arise from the mutual influence between spin carriers and a magnetized environment [1]. Both the potential technological applications and the research of new physical phenomena have strongly stimulated the study of spin-dependent transport in hybrid nanostructures. Assemblies of interacting and non-interacting magnetic nanoparticles in solids are attractive due to a rich variety of magnetic phenomena such as superparamagnetism [2], giant magnetoresistance [3,4], tunneling magnetoresistance [5-7], high-order magnetic tunneling [8], and because of their potential applications in high-density magnetic recording media [9,10], electromagnetic interference shielding and microwave absorbing applications [11]. The fundamental physics of the current-driven magnetization reversal has been studied in metallic trilayers [12] and tunnel junctions structures [13] envisaging its advantages over magnetization reversal using magnetic fields for future ultrahigh density magnetic memories [13].

The modeling of the electronic transport between magnetic particles embedded in a semiconducting or insulating matrix is complex, but it can be understood as a random ensemble of planar junctions interconnected, which implies that eventual short circuits are less detrimental and disastrous to the magneto-tunneling than in the magnetic tunnel junctions. The tunneling magnetoresistance (TMR) depends on the relative orientation of magnetizations between ferromagnetic particles. In these granular systems the tunneling process into a small grain or particle can increase the Coulomb energy by a charging effect that opens the Coulomb gap and enhances the tunnel resistance. This so called Coulomb blockade effect and was first observed by Abeles et al. in granular Ni-SiO_2 films [14]. Since there is a large number of particles with randomly oriented magnetic moments, the spin-dependent tunneling simultaneously with

Coulomb blockade effect is expected to cause magnetoresistive phenomena inherent to the granular structures [15-17].

We have found that metallic Co nanoparticles embed in a $TiO_{2-\delta}$ matrix can exhibit a surprisingly immense tunneling magnetoresistance (TMR) up to 300 % concomitantly with current-driven magnetization reversal. Cobalt is a ferromagnetic metal widely employed in the planar junctions and granular structures due to its high Curie temperature and high spin polarization (P_{Co} = 0.45) [18], whereas TiO_2 is a wide bandgap (3.1 eV) oxide semiconductor extensively studied for spintronics and optoelectronics applications since 2001 [19]. We describe here the preparation of such system as well as its magnetic, electric and magneto-electric properties. The high TMR has been observed for high applied bias voltage at low temperature associated with Coulomb blockade-assisted current-driven magnetization reversal.

Co clusters embed in $TiO_{2-\delta}$ thin films have been prepared by pulsed laser deposition from metallic Co and nominal $TiO_{2-\delta}$ targets with a base pressure around 10^{-7} mbar. An excimer KrF laser (λ=248nm, τ=20ns) with fluency of about 3 J/cm^2 and laser cadence around 2 Hz was used with a distance between substrate and target of 5 cm. Firstly, a 40nm-thick $TiO_{2-\delta}$ buffer layer was grown on the native thin oxide layer of a commercial Si(100) wafer. The Co granular film was grown at room temperature on the $TiO_{2-\delta}$ buffer layer, followed by a 40nm-thick overlayer of $TiO_{2-\delta}$. Rutherford Backscattering (RBS) and Transmission Electron Microscopy (TEM) were used to determine the oxide matrix composition and the film microstructure. The amorphous $TiO_{2-\delta}$ layers are nonstoichiometric with δ = 0.3. Transversal TEM micrographs of the granular $TiO_{2-\delta}$ – Co films are shown in Figure 1. The Co clusters display spheroidal shapes with diameters between 3 and 4 nm and intercluster distances of about 2 nm.

Magnetic analysis was carried out using a SQUID magnetometer (Quantum Design-MPMS-5S) with all measurements performed with the applied magnetic field parallel to the film surface. The magnetic evolution as a function of temperature was measured using zero-field cooling (ZFC) and field cooling (FC) protocols with temperature rate of 2 K/min.

Hysteresis loops measured at 1.8 K and 300 K are shown in Figure 2(a), with the inset showing the hysteresis curves normalized to saturation magnetization. Both coercive field (H_c= 300 Oe) and remanent magnetization (M_R=0.5) observed at low temperatures from the inset of Figure 2(a), are characteristic of a blocked state of the cluster magnetization. The M_R follows the expected behavior for non-interacting single domain particles with their magnetic moments randomly oriented. At high temperatures, an ideal superparamagnetic behavior is verified with an effective magnetic moment of about 12,000 μ_B according to the Langevin fitting. The ZFC-FC evolution shown in Figure 2(b) confirms the superparamagnetic behavior of a cluster assembly with the blocking temperature (T_B) at 30 K. The narrow peak in ZFC curve at T_B indicates that the clusters size distribution is small. By assuming the superparamagnetic response, the average volume of clusters can be estimated [20] from the equation $\langle V \rangle = 25 k_B T_B / K_{Co}$ in which k_B is the Boltzmann constant and K_{Co} is the Co anisotropy constant. Taking T_B = 30 K, $K_{Co} = 4.1 \times 10^6$ erg/cm^3 [21] and assuming the spherical shape of clusters we obtain an average diameter of 3.6 nm. This result is in very good agreement with TEM analyses. Above T_B, both ZFC-FC curves follow a Curie-Weiss law and the small magnetic irreversibility observed at low field (even at high temperatures) suggests that a weak magnetic coupling could occur between clusters.

Electric transport measurements were carried out in a Quantum Design PPMS-6000 system with an external voltage source, using the two-probe method. Silver epoxy was disposed directly on the $TiO_{2-\delta}$ capping layer to contact the sample. Figure 3(a) presents the resistance as a function of

temperature. A good agreement with an exponential resistance vs. temperature law is found at low temperatures, i.e. R(T) ~ *exp* (*-b/T*), indicating that the cluster size is monodispersed and the intercluster distance is uniform, as in the case reported in ref. 22. As discussed below, these characteristics are important to explain the immense TMR observed.

A broad distribution of cluster sizes and intercluster distances are frequently observed in such systems whose conduction obeys a $\exp(-b / T^{1/2})$ law at low bias. When the cluster size is monodispersed and the intercluster distance uniform, the conductance scales with $exp(-b/T)$ with $b = E_c/2k_B$ [15], where E_c is the electrostatic energy required to create a positive-negative charged pair in two clusters by tunneling and giving rise to the Coulomb blockade effect at low temperatures [22]. Thus, the result in Figure 3(a) indicates that the Co cluster size dispersion is small, corroborating TEM and magnetization measurements. The solid line is the best fit found with $b = 24.1$ K, i.e. $E_c \sim 4.1$ meV in good agreement with the calculated $E_c = (e^2 / 2\pi \varepsilon_0 \varepsilon d)[s / (d/2 + s)] \sim 4.5$ meV [15]. In the latter equation, e is the electron charge, $\varepsilon_0 = 8.854 \times 10^{-12}$ F/m is the vacuum dielectric constant, $\varepsilon = 80$ is de TiO_2 dielectric constant [23], $d = 4$ nm is the cluster diameter and $s = 2$ nm is the intercluster distance. This value of Ec indicates that above 50 K, when k_BT is larger than the Coulomb blockade electrostatic energy, the thermally-activated conduction of the system is restored.

The inset in Figure 3(a) shows non-linear current versus voltage curves at H = 0 Oe and 10 kOe. The current remains very small even at the highest applied voltage. Clearly, the magnetic field changes the current that flows into the system at large bias voltage indicating that a strong TMR is occurring.

Magnetoresistance has been measured at several bias voltages and temperatures. As a general behavior, it shows maximal values at low magnetic field range. Figure 3(b) presents a MR curve

measured at 5 K under bias voltages between 84.7 and 85.2 V. A surprisingly high TMR variation of about 300 % is observed calculated as TMR = $[(R_{max} - R_s) / R_s]*100$, where R_{max} is the maximum resistance and R_s is the resistance at the maximum applied magnetic field. This TMR value is by far larger than the expected value that is predicted by Jullière's model [24] for clusters without magnetic correlation (TMR = $P_{Co}^2/(1+P_{Co}^2)$). It is worthwhile to notice that high TMR values are found only for elevated bias voltages and that TMR maxima do not coincide with the coercive fields shown in Figure 2. For lower bias (not shown), TMR values are almost constant around ~ 5 % and the resistance maximas are coincident with the corresponding coercive fields. The small TMR variation with bias (low bias regime) is another signature [7,8] of the Coulomb blockade effect.

The apparently high bias voltage necessary to observe the enhanced TMR phenomena is a sum of a large number of effectively small voltages. In fact, since the resistance of our sample is measured with in-plane geometry, the voltage drop between two clusters (at one single tunnel junction) is effectively much smaller than the nominal applied voltage. In our particular case, the narrow cluster size distribution allows us to assume a common resistance value R_o for each junction. By taking a mean distance between contacts of about 3 mm and a junction as two clusters of 4 nm spaced by 2nm, one can roughly estimate a net chain containg around 10^5 junctions. Then, even at our voltage source limit of 100 V, the voltage drop between two clusters is low, i. e. ~ 0.4 mV. At temperatures satisfying $k_BT < E_c$ (i.e., below ~50 K) we are always working within the Coulomb blockade limit.

At this point it is interesting to address how tunneling conduction can occur in the blocked limit even though the effective voltage energy (eU) is small (below 50 K, $k_BT + eU < E_c$). It can be understood by making a parallel with the case of a single tunnel junction with low conductance: $R_o^{-1} << R_Q^{-1}$ ($R_Q \equiv h/4e^2 \approx 6.5$ kΩ). For the low conductance condition, the tunnel current is

suppressed for a low bias voltage, since tunneling would increase the Coulomb energy of the junction capacitance [25]. However, quantum fluctuations of the charge induce a non vanishing probability of quantum tunneling through the Coulomb energy barrier, and thus makes the zero-current Coulomb blockade state metastable. Only one electron is transferred through the junction by quantum tunneling. Nevertheless, electron transfers via quantum tunneling in small junctions is essentially a macroscopic process. This is because the tunneling electron polarizes the junctions in virtual states below the energy barrier, leading to a macroscopic electrostatic Coulomb energy. This implies that all free electrons of the junctions (where $k_BT + eU < E_c$) are expected to participate in the tunneling process. In this respect it is not the tunneling of a single electron but rather a macroscopic process involving the available electric charge q of the junctions.

Mitani et al [26] have observed a moderated enhancement of TMR (~ 20 %)associated with co-tunneling transport in Co-Al-O granular films with a large distribution of grain sizes. According to these authors, the anomalous increase of the TMR at low temperatures is produced by successive onset of high-order processes of spin-dependent tunneling between large grains via the small ones with strong Coulomb blockade, the co-tunneling. The enhancement of TMR arises from the fact that the probability of high-order tunneling is given by the product of the probability of each tunneling event [26].

In our case, however, the cluster size distribution is narrow as discussed above. We believe that at the energy given by the correct choice of temperature and bias voltage, a large amount of Co clusters can contribute to the high order co-tunneling transport in the Coulomb blockade regime. This can produce an enhancement of the TMR like the 300 % we have observed for Co on TiO_2. We would like to point out that this strong TMR value is, to our knowledge, the highest ever observed for granular systems.

However, at this point one should stress the importance of two experimental findings : (i) the TMR evolution with the applied bias voltage shown in Figure 3(b), where the switching fields of the TMR curves are not correlated with coercive fields; (ii) the magnetic field dependence of the step at U = 87 V in the current versus voltage curve shown in the inset of Figure 3(a). A possible mechanism sustaining these effects in our sample is that a cascade of polarized tunneling current densities, J, stimulate spin wave excitations or possibly flip the magnetic moment of individual clusters [27,28], i.e. a magnetization reversion mechanism. A rough estimation of the current density in our sample gives values as high as $J \sim 8 \times 10^8$ A/cm^2; where the effective area of a single junction is taken from a sphere with an average diameter of 3 nm and the current is $\sim 10^{-4}$ A (from the inset in Fig. 3(a)). This value is sufficiently large for spin-polarized tunneling currents be able to flip the magnetization of an isolated particle, as predicted by Slonczewski [27].

To examine this point we investigate this spin transfer effect in our sample by polarizing it electrically during magnetization measurements. In Figure 4 we show the magnetic moment measurement as a function of the applied bias voltage with electrical polarization along the magnetizing field direction for three different values of the magnetic field. Clearly, the magnetization evolution with applied bias voltage promotes a rearrangement of the magnetization of the sample as a whole. The magnetization of the sample appears strongly dependent of the applied fields and voltages above 84 V. We note that even a full reversal of the saturation magnetization of the sample can be achieved. For measurements at positive 10 kOe lying along the +z direction and zero bias (inset in Fig. 4) the sample presents a total magnetic moment of + 7.63×10^{-6} emu. By applying U = 100 V along the same +z direction, the magnetization reversal takes place, even though the magnetic field of 10 kOe is kept in the +z direction, and the total magnetic moment measured is negative and equal to - 7.14×10^{-6} emu. While the magnetization

direction depends on the applied bias, the magnetizing field can amplify or attenuate the magnetization reversal driven by the moment transferred by the current. A recent work by Chiba et al. [13] supports our results demonstrating that current-driven magnetization reversal is possible in magnetic tunnel junctions. The spin-polarized tunneling between isolated magnetic particles with flip or precession of their magnetization (and corresponding damping) is a complex subject and is not totally understood at this moment. However, the dependence of the hysteretic resistance switching on the bias voltage observed in our sample constitutes a strong evidence that a spin-transfer mechanism and not the Oersted fields created by the current flow is responsible for the effect.

In conclusion, we have successfully grown Co clusters embedded in $TiO_{2-\square}$ matrix by pulsed laser deposition. The sample presented Co particles with average diameter of about 4 nm that are well separated from each other by 2-nm-thick $TiO_{2-\delta}$ barrier with small deviations according to magnetic and electric analyses. From the magnetic results we observed a nearly ideal superparamagnetic like behavior. Electronic transport measurements shown that Coulomb blockade effect plays an important role in the observed phenomenon. Most importantly, we demonstrate that, for magnetic nanoparticles embedded in an insulating matrix, the interplay between Coulomb blockade effect and current-driven magnetization reversal from a spin-polarized tunneling current produces an immense TMR variation of 300%. The correct tuning of competing experimental parameters such as thermal energy, bias voltage and magnetic field, with respect to the Coulomb energy, is essencial to activate the immense TMR variation observed. Work is in progress to further characterize these granular systems and so to improve the understanding about the role of the local electronic structure of the interfaces in the tunneling process.

The authors would like to tank A. Fert for the critical reading of this paper. This work was supportted by Brazilian Agencies CNPq, FAPESP (grants 03/09933-8 and 04/08524-0) and resources for this international cooperation granted by CAPES (Brazil) and COFECUB (France).

References

[1] S. A. Wolf *et al.*, Science 294, 1488 (2001)

[2] C. L. Chien, J. Appl. Phys. 69, 5267 (1991)

[3] A. E. Berkowitz *et al.*, Phys. Rev. Lett. 68, 3745 (1992)

[4] J. Q. Xiao, J. S. Jiang, C. L. Chien, Phys. Rev. Lett. 68, 3749 (1992)

[5] H. Fujimori, S. Mitani, S. Ohmuna, Mater. Sci. Eng. B 31, 219 (1995)

[6] J. Inoue, S. Maekawa, Phys. Rev. B 53, R11927 (1996)

[7] B. Hackenbroich, H. Zare-Kolsaraki, H. Micklitz, Appl. Phys. Lett. 81, 514 (2002)

[8] S. Mitani *et al.*, Phys. Rev. Lett. 81, 2799 (1998)

[9] J. F. Gregg *et al.*, J. Phys. D: Appl. Phys. 35, R121 (2002)

[10] V. Skumryev *et al.*, Nature 423, 850 (2003)

[11] M. T. Nguyen, A. F. Diaz, Adv. Mater. 6, 858 (1994)

[12] J. Grollier et al., Phys. Rev. B **67**, 174402 (2003)

[13] D. Chiba et al., Phys. Rev. Lett. **93**, 216602 (2004)

[14] B. Abeles *et al.*, Adv. Phys. 24, 407 (1975)

[15] D. L. Peng *et al.*, Phys. Rev. B **60**, 2093 (1999)

[16] L. F. Schelp et al., Phys. Rev. B **56**, R5747 (1997)

[17] H. Zare-Kolsaraki and H. Micklitz, Phys. Rev. B **67**, 224427 (2003)

[18] J. S. Moodera and S. Mathon, J. Mag. Mag. Mat. **200**, 248 (1999)

[19] Y. Matsumoto *et al.*, Science **291**, 854 (2001)

[20] C. L. Chien, J. Appl. Phys. **69**, 5267 (1988)

[21] C. Kittel, Introduction to Solid State Physics, seventh edition, Wyley 1996

[22] P. Sheng, B. Abeles and Y. Arie, Phys. Rev. Lett. **31**, 44 (1973)

[23] S. A. Campbell *et al.*, IBM J. Res. Develop. **43**, 383 (1999). *In reality, the TiO_2 dielectric constant is very dependent on the deposition conditions, and interfaces. The value utilized is an average value between those found in the literature.*

[26] J. Inoue and S. Maekawa, Phys. Rev. B **53**, R11927 (1996)

[25] L. J. Geerligs, D. V. Averin and J. E. Mooij, Phys. Rev. Lett. **65**, 3037 (1990)

[26] S. Mitani *et al.*, J.Mag. Mag. Mat. **198-199**, 179 (1999)

[27] J. Slonczewski, J. Magn. Magn. Mater. 159, L1 (1996)

[28] L. Berger, Phys. Rev. B 54, 9353 (1996)

Figure Captions

Figure 1 – Cross-sectional TEM image of the Co clustered film in the $TiO2_{-\delta}$ matrix.

Figure 2 – (a) Magnetic moment measured at 1.8 and 300 K as a function of the applied magnetic field. The inset shows the inner part of the loops. (b) ZFC-FC magnetization curves measured at 50 Oe. The magnetic field was applied parallel to the film surface.

Figure 3 – (a) Resistance versus inverse temperature measured at 10 V. The solid line is an adjustment with *exp(b/T)*-law expected for a narrow cluster size distribution. The inset shows current versus voltage curves measured at 5 K in zero field and 10 kOe. (b) Tunnel magnetoresistance measured at 5 K at relevant applied bias voltages.

Figure 4 – Relative variation of the normalized magnetization as a function of the applied bias voltage at fixed magnetic fields of 1, 5 and 10 kOe. Measurements were performed at 5 K with electrical polarization along the applied magnetic field as shown in the inset.

Varalda et al., Figure 1.

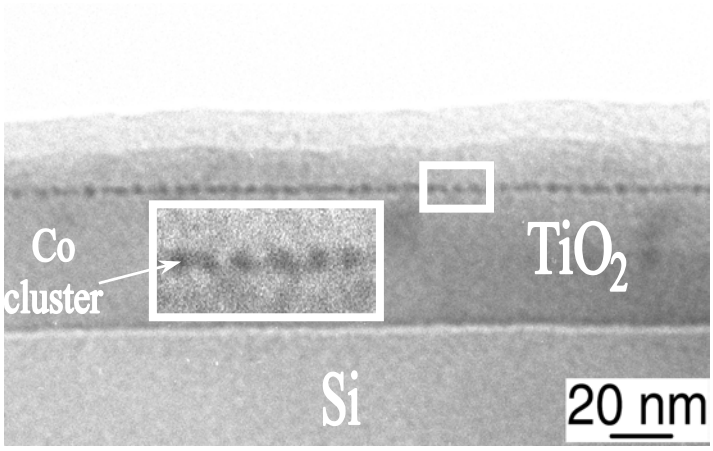

Varalda et al., Figure 2.

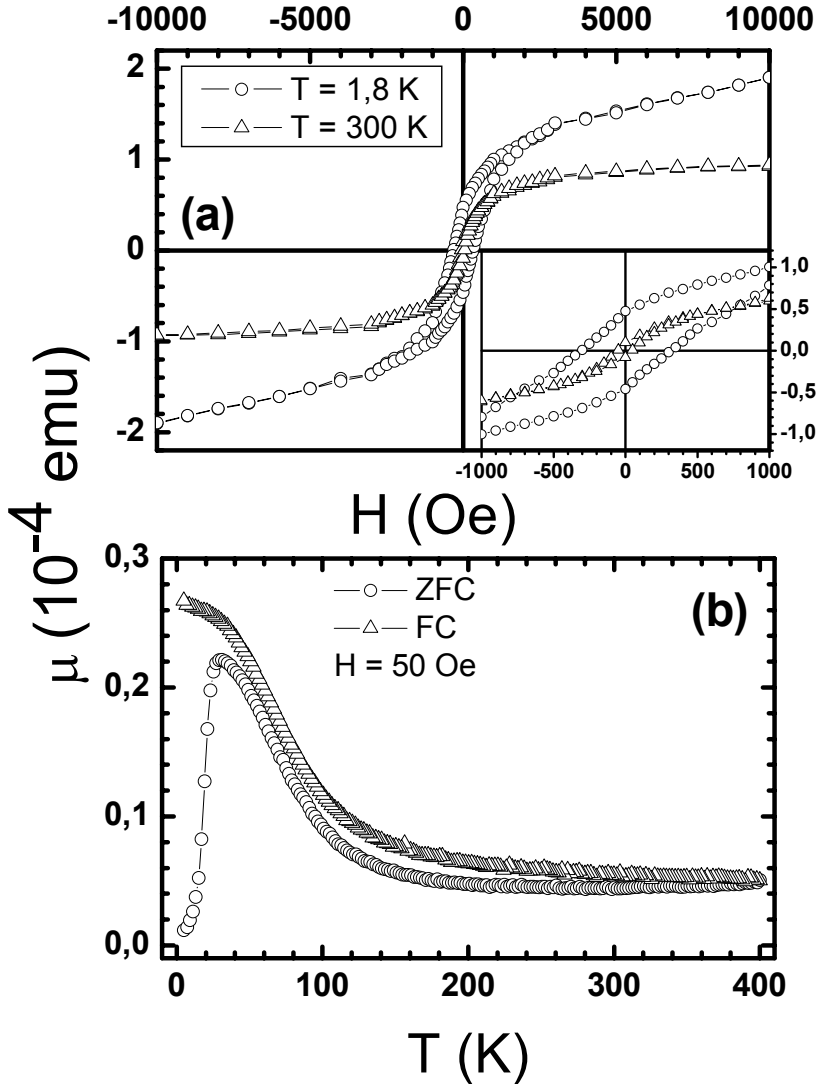

Varalda et al. , Figure 3.

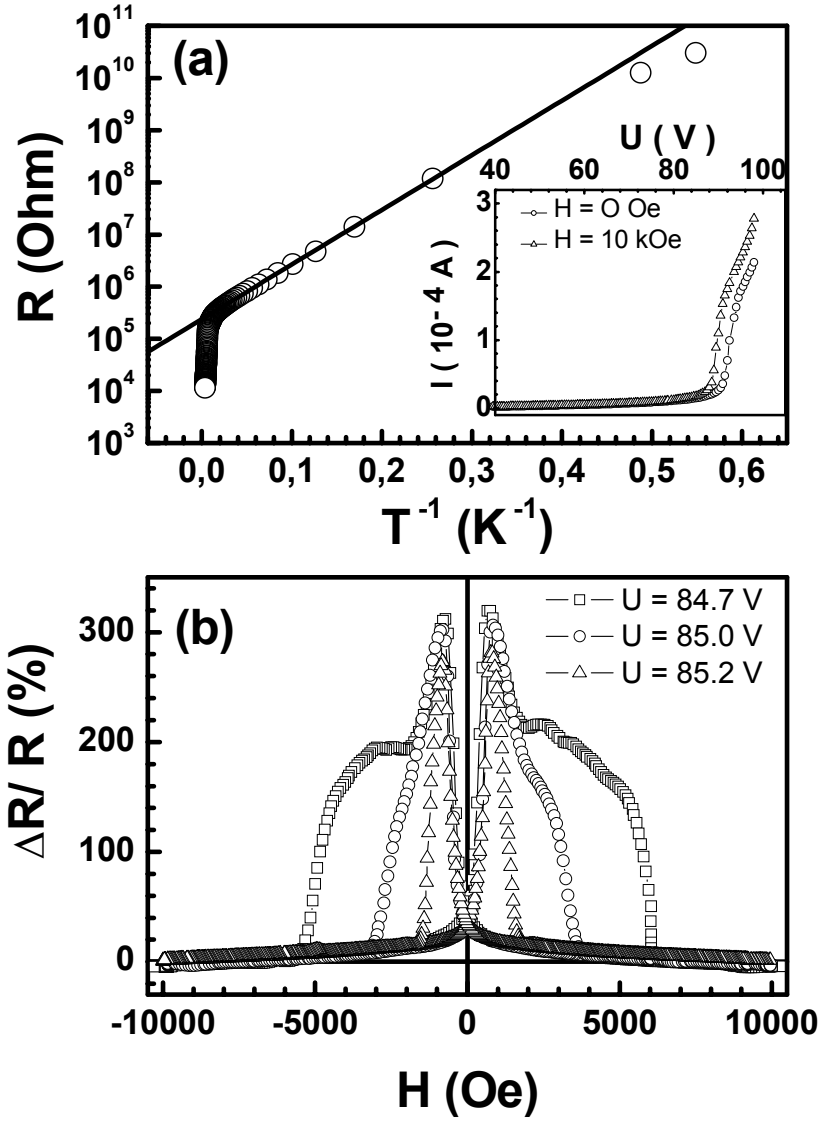

Varalda et al. , Figure 4.